Original Article

DOI: 10.5582/ddt.2025.01000

Emulsification-based liposomal formulation of gallic acid and curcumin as potent topical antioxidants

Takron Chantadee[1,2,3], Siripat Chaichit[1], Kanokwan Kiattisin[1], Worrapan Poomanee[1], Siriporn Okonogi[1,2], Pimpak Phumat[1,2,*]

[1] Department of Pharmaceutical Sciences, Faculty of Pharmacy, Chiang Mai University, Chiang Mai, Thailand;
[2] Center of Excellence in Pharmaceutical Nanotechnology, Chiang Mai University, Chiang Mai, Thailand;
[3] Natural Bioactive and Material for Health Promotion and Drug Delivery System Group (NBM), Faculty of Pharmacy, Silpakorn University, Nakhon Pathom, Thailand.

SUMMARY: Excessive free radicals in the skin cause oxidative stress, damaging cells and leading to aging, melasma, and inflammation. This study developed a liposome system for co-delivering antioxidants to enhance their efficacy in deeper skin layers. Four phenolic compounds were screened for antioxidant activity using DPPH, nitric oxide scavenging, and lipid peroxidation assays. Gallic acid and curcumin, showing the strongest activity, were selected for liposome encapsulation *via* an emulsification method, with particle size reduction by probe sonication. High-performance liquid chromatography (HPLC) was used for chemical analysis, and particle morphology was examined with transmission electron microscopy. Studies on skin penetration, retention, and release were conducted. The optimized liposome (LP4) had a small particle size (< 150 nm), an unilamellar structure, and high entrapment efficiency (99% gallic acid and 92% curcumin). LP4 promoted effective skin retention of curcumin with slow penetration, while the release of gallic acid and curcumin from LP4 followed a Higuchi kinetic model and Zero-order kinetic model, respectively. This delivery system demonstrates potential for targeted antioxidant delivery, offering enhanced protection against oxidative damage in the skin.

Keywords: gallic acid, curcumin, liposome, skin penetration, kinetic releasing

1. Introduction

Oxidative stress is a condition that exists an imbalance of the production of radicals and a neutralized mechanism of these radicals, including reactive oxygen species (ROS) which are hydroxyl radical ($OH^{\bullet}$), superoxide ($O2^{\bullet-}$), and peroxyl radical ($ROO^{\bullet}$), as well as reactive nitrogen species (RNS) (*1*). An excess of free radicals can damage cells and various systems, resulting in protein modification, genetic alterations, and trigger inflammation (*2,3*).

Skin, a primary barrier that functions against the external factors that can elevate free radical levels within the body, including environmental pollutants, ultraviolet (UV) radiation from sunlight. Free radicals in the skin induce inflammation and damage cells in deep skin layers such as fibroblasts, keratinocytes in dermis layer that resulted in skin aging, leading to abnormal pigmentation, and reduced skin barrier functions (*4*). The continuous skin damaged by radicals can lead to chronic skin inflammations like seborrheic dermatitis and eczema and damaging cellular structures, including deoxyribonucleic acid (DNA), proteins, and lipids in dermal cells, ultimately impairing skin function and accelerating aging processes. The substances that function as antioxidants thus play a crucial role in reducing these harmful effects on the body (*5*).

Phenolic substances are found in many kinds of plants which are widely recognized as potential antioxidant properties, have gained substantial attention in pharmaceutical and cosmetic applications. Their chemical structure consists of a benzene ring with at least one hydroxyl group (OH), that grants antioxidant properties by neutralizing free radicals and thereby mitigating oxidative stress and cellular damage (*6,7*). The structural differences among phenolic substances result in varying physicochemical properties and lead to constrain of their applications by poor solubility, instability, and limited skin penetration. Various studies have been reported on the antioxidant and anti-inflammatory properties of phenolic substances, which are used to prevent and reduce skin inflammation. Antioxidants have garnered significant attention in the cosmetic and pharmaceutical industries due to their

potential to alleviate skin damage and promote healthy aging (*8*). Gallic acid (GA), a hydrophilic phenolic compound that possesses strong antioxidative activity with various mechanisms (*9*). Lipophilic phenolic compounds which are curcumin (Cur), a polyphenolic compound major found in turmeric, kaempferol (Kaf) which is a flavonoid that generally found in tea, broccoli, cabbage, kale, beans, and sesamin (Sem) a lignan substance found in sesame seeds have been reported as the potential antioxidants and anti-inflammatory agents (*10–12*). However, the skin permeation through the skin's lipid-rich barrier of those compounds is often limited due to their physicochemical properties such as hydrophilic-lipophilic properties, molecular size, structural complexity, including chemical instability (*13*).

Liposomes have been extensively explored as promising delivery system for hydrophobic and hydrophilic substances. These spherical vesicles, composed of lipid bilayers, facilitate the entrapment and penetration of active compounds into deeper skin layers while allowing controlled release (*14*). The encapsulation of hydrophobic or lipophilic substances in liposomes not only enhances their solubility but also protects them from degradation and improves their overall stability. Encapsulating phenolic compounds in liposomes significantly increases their solubility, enhances skin penetration, and improves their stability (*15*). This delivery method enables more effective targeting of desired sites, thereby augmenting their biological activities, including their antioxidative effects (*7*).

It is therefore interesting to investigate and compare the antioxidative activities of potential substances with different physicochemical properties which are GA, Cur, Kaf, and Sem. Subsequently, the two substances exhibiting the strongest antioxidant activity will be selected to develop substance-encapsulated liposomes as innovative carriers for promising antioxidant delivery through the skin and application in cosmetic formulations.

2. Materials and Methods

2.1. Materials

The reagents and chemicals were of analytical grade. 2,2-Diphenyl-1picrylhydrazyl (DPPH) and GA from Fluka (Werdenberg, Buchs, Switzerland). Ascorbic acid, β-carotene, linoleic acid. tocopheryl acetate from Glentham Life Sciences (Planegg, Munich, Germany). Cur, Kaf, and Sem purchased from Greenway (Nanjing, Jiangsu, China). Phosphate buffer was from HiMedia (Kennett square, Pennsylvania, USA). Sodium nitroprusside (SNP), N-(1-Naphthyl) ethylenediamine dihydrochloride, phosphotungstic acid were from Kemaus (Cherrybrook, New south wales, Australia). Hydrogenated lecithin and cholesterol from Nikko Chemicals (Pulau Seraya, Jurong island, Singapore). Ethylhexyl palmitate, ethylhexyl glycerin dipropylene glycol, polysorbate 80, and sorbitan were from BASF (Ludwigshafen, Rhineland-Palatinate, Germany). Phenoxyethanol from Seppic (La-Garenne Colombes, Paris, France). Phosphotungstic acid from QRëC (Mueang, Chonburi, Thailand). Absolute ethanol, chloroform, methanol from RCI Labscan (Pathumwan, Bangkok, Thailand).

2.2. Determination of antioxidant activity

2.2.1. DPPH assay

This experiment followed a modified method from previous study (*16*). A total of 20 µL of the phenolic substance solution (ranging from 1 to 10,000 µg/mL) that dissolved in absolute ethanol was mixed with 180 µL of DPPH reagent (1.0 M^{-4}) in 96-well plate and incubated in the dark at an ambient temperature for 30 min. Then, the plate was subjected to analyzed using a microplate reader (SPECTROstar Nano, BMG Labtech, Ortenberg, Germany) at the wavelength 520 nm. The antioxidant activity against DPPH radicals was expressed as the percentage of inhibition (% inhibition), calculated using the following equation:

$$\% \text{ Inhibition} = [(Ap - An) - (At - Ad/(Ap - Ar)] \times 100$$

where Ap, An, At, Ar were the absorbances of reagent mixed with diluent, diluent of test sample, tested samples mixed with reagent, and the tested samples mixed with diluent of sample, respectively. Ascorbic acid was used as positive control in comparison.

2.2.2. Nitric oxide (NO) scavenging assay

NO scavenging assay was carid out using Griess test following method of Jagetia with some modification (*17*). A total of 20 µL of the phenolic substance solution (ranging from 1 to 10,000 µg/mL) was added in 96-well plate, followed by adding 60 µL of 10 mM SNP, 20 µL of PBS pH 7.4 and incubated in the dark at an ambient temperature for 150 min. After that, 50 µL of 1% w/v sulfanilamide dissolved in 2% v/v phosphoric acid was added in the tested mixture and continuously incubated in the same condition for 5 min. Then, 50 µL of *N*-(1-naphthyl) ethylenediamine dihydrochloride was added and incubated at 25°C for 10 min. The solution mixtures were measured the nitrite concentration at 540 nm by microplate reader. The activity against NO radicals of the tested samples was expressed as the percentage of scavenging (% scavenging), calculated using the following equation:

$$\% \text{ Scavenging} = [(As - Ab) - (Aw - Ao)/(As - Ab)] \times 100$$

where As, Ab, Aw, Ao were the absorbances of SNP

mixed with diluent; ethanol or DI water and PBS (positive control), diluent (negative control), tested samples mixed with SNP and PBS, sample mixed diluent and PBS, respectively. Ascorbic acid was used as positive control in comparison.

2.2.3. Lipid peroxidation inhibition assay

This study was evaluated β-carotene bleaching inhibitory ability following the method of Elzaawely with some modification (*18*). β-carotene emulsion was prepared by mixing of β-carotene solution in chloroform (2,000 µg/mL) with 200 mg of Tween 20 and 20 mg of linoleic acid. The mixture was then allowed to stand for removal of chloroform using evaporator (MA3S, Eyela, Tokyo, Japan) and a thin film was obtained. Then, adding 50 mL of DI water, the mixture was subjected to shaking, which resulted in the formation of self-emulsion. The emulsion (180 µL) was combined with a sample (20 µL) in 96-well plate. The absorbance was determined at 470 nm at 0, 30, 60, 90, and 120 min. The β-carotene bleaching inhibitory activity of a sample was assessed following equation as shown in 2.2.1.

2.3. High-performance liquid chromatography (HPLC) analysis

The qualitative analysis of GA and Cur was done by using an isocratic HPLC system using an Agilent Eclipse XDB-C18 (4.6 × 150 mm) HPLC column and analyzed on a Shimadzu Prominence HPLC systems (Nakagyo-ku, Kyoto, Japan). The mobile phase consisted of methanol (A) and 1% phosphoric acid in DI water (B) in a ratio of 70%-90% A and 10%-30% B, the flow rate was 0.7 mL/min for 15 min, and the injection volume was 10 µL. The detection wavelength was 280 nm. Mixed GA and Cur solution was used as the sample to investigate the suitable mobile phase ratios for HPLC condition. An intact GA and Cur diluted at a concentration range of 0-500 µg/mL was subjected to the HPLC at the same condition to construct a linear standard curve. All the samples were prepared by dissolved in methanol and filtered through 0.45 µm before analysis.

2.4. Development of liposomal formulations

The preparation was first prepared the primary emulsion. The lipid phase which consists of hydrogenated lecithin, cholesterol, ethylhexyl palmitate and/or ethylhexyl glycerin, dipropylene glycol, tocopheryl acetate, sorbitan oleate, and phenoxyethanol were weighed in the same beaker and mixed with gentle agitation at 60°C for 15 min and the mixer was presented as a clear mixture. An aqueous phase was prepared by dissolving polysorbate 80, sorbitan oleate in DI water with gentle agitation under 60-63°C for 15 min and the mixture showed a clear solution. Subsequently, the lipid and aqueous phases were mixed to obtain liposome primary emulsion, which is then homogenized using a high-shear homogenizer T 25 digital ULTRA-TURRAX® IKA (Breisgau-Hochschwarzwald, Staufen, Germany) at a speed of 7,000 rpm for 15 min to produce a uniform emulsion. Then, particle size was reduced by using probe sonicator (VCX 600, Sonics & Materials, Newtown, Connecticut, USA) at 65% intensity for 15 min with an alternating on-off pattern every 1 second under temperature below 20°C to prevent excessive heat production during the process of size reduction.

2.5. Viscosity study

The viscosity value of each formulation was carried out using a plate and plate rheometer (R/S Brookfiled, Massachusetts, USA). A sample volume of 1-3 g was evaluated with the shear rate ranging from 1-60 s^{-1} for 120 s; at 25 ± 2°C. Brookfield Rheocalc operating software was used to analyze.

2.6. Investigation of particle size and zeta potential

The liposomal particles were investigated the size, size distribution, and zeta potential using a Zetasizer (Malvern, Worcestershire, UK). The sample was diluted 100-fold to 1,000-fold in DI water before analysis, then subjected to the Zetasizer and detected at a fixed angle of 173° at 25°C for size and size distribution. A size distribution was expressed as a polydispersity index (PdI) value. Zeta potential of the particles was also examined using Zetasizer ant 25°C. All measurements were performed in triplicate.

2.7. Entrapment efficiency

For sample preparation, liposomal encapsulated substance formulation was firstly diluted in DI water to 2-fold and then 0.5 mL of diluted sample was centrifuged at 10,000 rpm at 25°C for 30 min using Amicron Ultra (50 kDa) – 0.5 mL centrifugal filters (Merck Millipore Ltd., Carrigtwohill, Cork, Ireland) to separate free substance and liposomal encapsulation. Then, the unentrapped substance (free substance) was quantified using HPLC, and entrapment efficiency (EE) was expressed as percentage (%) and calculated as equation:

$$\% EE = (Co - Cf/Co) \times 100$$

where Co is the total amount of loaded substance and Cf is amount of free substance.

2.8. Liposomal morphology

Transmission electron microscopy (TEM) was used to investigate the morphology of the selected liposome formulation. The formulation was diluted 100-fold with

DI water and analyzed using a TEM JEM-2010 (JEOL, Akishima, Tokyo, Japan) operating at an acceleration voltage of 100 kV. For sample preparation, 10 µL of diluted formulation was carefully dropped onto a 200-mesh copper grid coated with formvar and carbon (FCF-200 mesh Cu, Electron Microscopy Sciences, Hatfield, Pennsylvania, USA) and the sample was allowed to air-dry for 5 min. Excess solution was removed using filter paper and the sample was then stained with a 3% (w/v) phosphotungstic acid solution. After 5 min, the excess staining solution was removed with filter paper. The prepared grid was allowed to dry at an ambient temperature at least 24 h, it was then subsequently subjected into the TEM for analysis.

2.9. Kinetic releasing study

The release of GA and Cur from selected liposome formulation were determined by a dialysis method modified from our previous study (*19*). The release kinetic was analyzed according to Zero-order, First-order, Higuchi model and Korsemeyer-Peppas model. The GA and Cur without loading in liposomes (free form) were used in comparison. PBS pH 7.4 mixed 0.5% w/v Tween 80 was used as releasing medium. 1 mL of LP7 was pipetted into a pre-swollen dialysis bag (regenerated cellulose membrane with MWCO of 12,000). The dialysis bag was tightly closed and immersed into 20 mL of the release medium with stirring at 100 rpm at 37 ± 2°C. Samples (1 mL) of the release medium were drawn peri-odically at time interval of 5, 15, 30, 60, and 120 min. Fresh medium with the same volume was added into the dissolution medium after each sample withdrawal. The amount of GA and Cur was determined by HPLC as described above. The percentage cumulative release of GA and Cur which were the loaded substances at time T (Rt) was calculated using the following equation:

$$Rt = (Rt/Ro) \times 100\%$$

where Rt is the cumulative concentration of loaded substances released in the release medium at time t and Ro is the initial amount loaded substances in liposome. The results obtained were analyzed for drug release kinetics using Microsoft Excel version 2409.

2.10. Skin penetration and skin retention studies

This study was conducted using Franz diffusion cell method modified from the previous study (*20*). The Franz diffusion cell diffusion system (V9-CA, PermeGear Inc., Hellertown, Pennsylvania, USA) composed a diffusion area of 1.77 cm^2, receptor medium capacity of 12 mL which was PBS pH 7.4 and operated under a constant temperature of 37 ± 0.5°C *via* thermostatic bath circulation. The receptor medium was stirred constantly at 350 rpm during the experiments. A porcine membrane was used as a membrane model in this experiment. The 1 mL of tested samples; mixed intact GA-CUR solution and liposomal GA-CUR formulation were placed in donor chamber, and 1 mL of medium from receptor chamber was sampling at 15, 30, 60, 90, 120, 240, 360, and 480 min, then replaced by a fresh medium with an equal volume to maintain the sink condition throughout the investigation. The collected samples were analyzed using HPLC.

The formulation remained on the surface membrane after the end of skin penetration experiment was subsequently removed by washed repeatedly with deionized water. The membrane was then cut into small pieces and extracted with methanol using a sonication bath for 10 min. The quantitative of GA and Cur, the sample extracted from the membrane were analyzed by HPLC. All measurements were performed in triplicate.

2.11. Statistical analysis

All results are presented as mean ± standard deviation (n = 3). Statistical analysis was conducted using SPSS software version 17.0 for Windows. The group differences were investigate using one-way analysis of variance (ANOVA), followed by Tukey's post-hoc test. A P-value ≤ 0.05 was considered to statistical significance.

3. Results

3.1. Antioxidative activities of potential phenolic substances

The antioxidative property of potential phenolic substances that were selected in this study (GA, Cur, Kaf, Sem) were determined in comparison using various mechanisms of testing. Ascorbic acid was used as a positive control of all methods. The results are shown in Table 1.

DPPH assay was performed to assess the potential of the tested sample in scavenging activity against OH^- radical generated from DPPH reagent. The results were expressed as the concentration of the tested sample that could inhibit the generated radicals as 50% (IC_{50}). The IC_{50} values were calculated from the regression equations of each sample. Ascorbic acid possessed the highest activity with IC_{50} of 0.78 ± 0.10 µg/mL. GA exhibited the highest inhibitory activity compared to other tested samples, with the significantly lowest IC_{50} of 2.37 ± 0.32 µg/mL ($P < 0.05$), followed by Cur and Kaf. While Sem did not show the activity at the tested concentration (1,000 µg/mL).

NO scavenging assay was conducted to evaluate the potential of the tested samples in neutralizing RNS or NO radicals which are unstable and typically present under aerobic conditions. The results were expressed as the scavenging concentration required to achieve 50% inhibition of NO radicals (SC_{50}). The SC_{50} of these tested

Table 1. Screening of antioxidant activity with various mechanisms obtained from four phenolic substances

Samples	DPPH assay IC_{50}* (µg/mL)	NO assay SC_{50}* (µg/mL)	Lipid peroxidation inhibition assay % Inhibition* after 2 h (Sample concentration of 10 µg/mL)
GA	2.37 ± 0.32^{b}	943.0 ± 2.91^{c}	94.44 ± 0.00^{a}
Cur	11.77 ± 0.40^{c}	70.0 ± 0.02^{b}	59.26 ± 2.61^{c}
Kaf	10.64 ± 0.26^{c}	$> 1{,}000^{d}$	31.48 ± 6.93^{d}
Sem	$> 1{,}000^{d}$	$> 1{,}000^{d}$	88.89 ± 4.53^{b}
Ascorbic acid	0.78 ± 0.10^{a}	40.0 ± 0.00^{a}	37.04 ± 6.93^{d}

*Lowercase letters indicate significant differences ($P < 0.05$) in each assay.

samples were calculated from the obtained regression equations. It was shown that Cur possessed the highest activity with SC_{50} of 70.0 ± 0.02 µg/mL significantly ($P < 0.05$), followed by GA. Kaf and Sem not presented the activity with the tested concentration (1,000 µg/mL).

β-Carotene bleaching procedure was employed to explore the antioxidant potential through lipid peroxidation mechanism. Antioxidant activity is measured by the stability of the orange color of β-carotene over time against free radicals generated in DI water, a reaction medium, which can degrade β-carotene molecules. The inhibition of β-carotene bleaching is expressed as % Inhibition. The results found that GA possessed the highest inhibition (88%), followed by Sem, Cur, ascorbic acid, and Kam, respectively.

These experiments could conclude that GA and Cur provide a potential antioxidant activity after compared to other samples. Thus, GA and Cur were selected to develop the liposome system.

3.2. HPLC analysis

HPLC conditions were trial with various ratios of mobile phase to obtain GA and Cur peaks under operation using single condition. The suitable ratio of mobile phase contained methanol and 1% PA solution in a ratio of 70:30 which provided a separate HPLC peak of GA and Cur as shown in Figure 1 at the retention time of 2.16 min and 6.53 min, respectively. The GA and Cur quantitative determination along the study were calculated from the linear equations obtained from HPLC analysis following y = 104632 + 653876 of standard GA solution (R^2 = 0.9993) and y = 57880x + 260716 of standard Cur solution (R^2 = 0.9997).

3.3. Liposomal formulations

In the formulations, hydrogenated lecithin was employed as a vesicle membrane (shell), cholesterol could stabilize membrane, ethylhexyl palmitate, ethylhexyl glycerin, and dipropylene glycol were solubilizing agents, tocopheryl acetate used as antioxidants of system, polysorbate 80 and sorbitan oleate were the surfactants, and phenoxyethanol used as a preservative. The liposomal vesicles were self-assembly forming upon mixing of lipid and aqueous phases. The particle size was

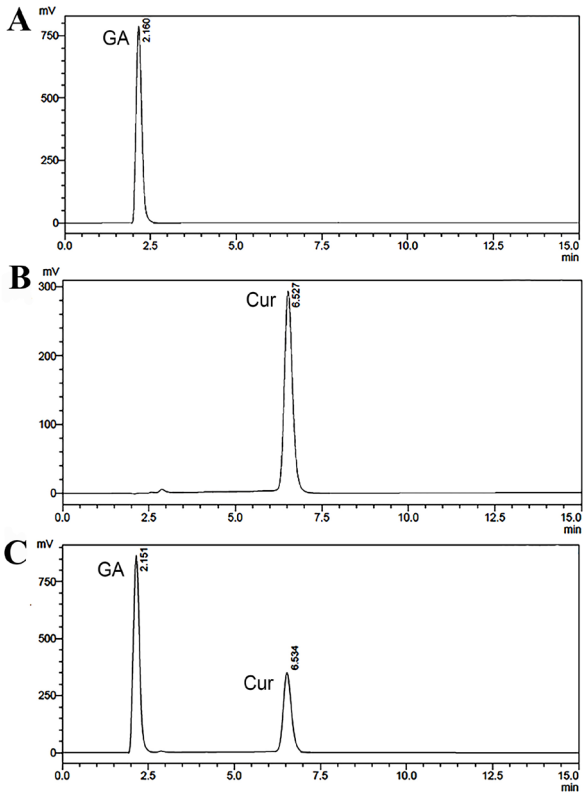

Figure 1. HPLC chromatograms. (A) GA peak at RT of 2.1 min, (B) Cur peak at RT of 6.5 min, and **(C)** HPLC peaks of GA and Cur of mixed solution, analysis at 280 nm.

extensively reduced by ultrasound force.

The formulations were developed by varying the percentages of hydrogenated lecithin, surfactants, cholesterol, and ethylhexyl palmitate as shown in Table 2. The outer appearance of the formulations, as shown in Figure 2, was observed through visual analysis. Blank liposomal formulations (LB) were initially prepared and characterized. It was found that high concentrations of hydrogenated lecithin (LB1 and LB2) affected the turbidity of the formulations. LB1 and LB2 were more translucent than the others. However, phase separation was observed in LB1 after 24 h, whereas LB2 was homogenized and thickened to a cream-like appearance. LB3 was subsequently developed from LB2 by reducing the hydrogenated lecithin content. The appearance of LB3 exhibited increased fluidity with white opacity. Subsequently, LB4 was developed by reducing

Table 2. Composition of blank liposome (LB) and GA-Cur co-loaded in liposome (LP) formulations

Composition	Formulation (% w/w)							
	LB1	LB2	LB3	LB4	LP1	LP2	LP3	LP4
Hydrogenated lecithin	2	2	1	0.5	2	2	1	0.5
Cholesterol	0.4	0.4	0.4	0.2	0.4	0.4	0.4	0.2
Ethylhexyl palmitate	10	10	10	5	10	10	10	5
Ethylhexyl glycerin	6	-	-	-	6	-	-	-
Dipropylene glycol	5	5	5	2.5	5	5	5	2.5
Tocopheryl acetate	1	1	1	1	1	1	1	1
Polysorbate 80	8	16	16	8	8	16	16	8
Sorbitan oleate	10	20	20	10	10	20	20	10
Cur	-	-	-	-	0.5	0.5	0.5	0.5
GA	-	-	-	-	0.5	0.5	0.5	0.5
Phenoxyethanol	0.5	0.5	0.5	0.5	0.5	0.5	0.5	0.5
Water	58.1	44.1	45.1	72.05	58.1	44.1	45.1	72.05

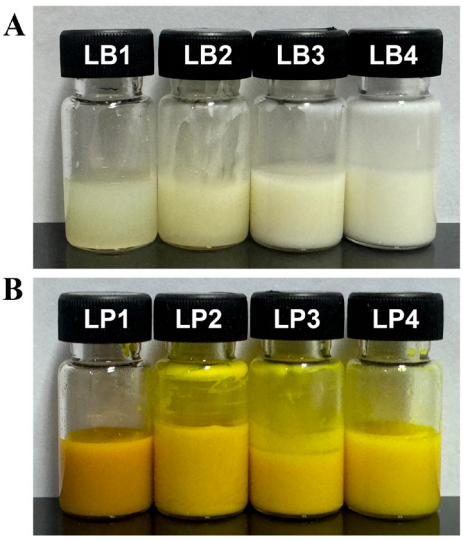

Figure 2. The appearance of liposomal formulations. (A) blank liposome (LB1- LB4) and **(B)** GA-Cur loading in liposome (LP1 – LP4).

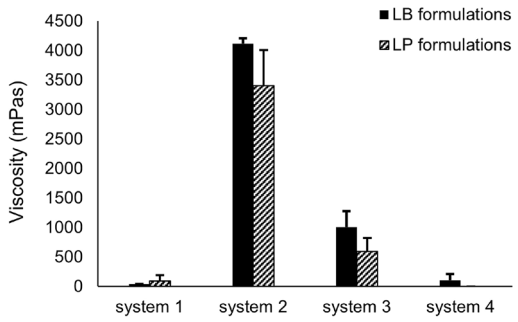

Figure 3. Viscosity of liposomal formulations. Comparison of viscosity between LB and LP formulations for all systems.

the amounts of hydrogenated lecithin, cholesterol, ethylhexyl palmitate, and surfactants used from LB3. This formulation displayed fluidity and white turbidity like milk. Each GA and Cur were incorporated at a concentration of 0.5%. GA was prepared in the aqueous phase, while Cur was prepared in the lipid phase. The appearance of GA-Cur loaded liposomes (LP) was turbid yellow in color, and the fluidity was similar to that of the LB formulations. Insistingly that LP4 exhibited the most stable formulation with a homogeneous appearance.

3.4. Viscosity study

The formulations with and without GA and Cur loading were investigated in comparison. The results were demonstrated in Figure 3. In LB formulations, almost all systems demonstrated higher viscosity compared to their LP in the same system, except for System 1. The LB1 exhibited lower viscosity than the LP1, possibly due to phase separation. System 2 showed the highest viscosity, with values of 4,113.72 ± 97.35 mPas for LB2 and 3,408.96 ± 600.42 mPas for LP2. System 4, which exhibited fluidity, showed low viscosity in LB4 with a value of 104.84 ± 152.19 mPas, whereas the viscosity value could not be determined for LP4.

3.5. Determination of particle size analysis and %EE

The results of particle analysis obtained from Zetasizer that demonstrated in Table 3 were expressed in size, size distribution with polydispersity index (PdI), and zeta potential (ZP) that indicated the trending of stabilized particles. The liposomal particles of LB formulations demonstrate smaller size than the particles of LP which contained GA and Cur in system. The particle size of LB was in a range of 51.53 ± 0.12 to 223.87 ± 16.05 nm whereas the particle size of LP was in a range of 130.07 ± 0.40 to 804.27 ± 74.71 nm. PdI value of formulations varied from 0.24 to 0.90 for LB formulations and in a rage of 0.16 to 0.69 for LP formulations. ZP of LB and LP formulations were a negative charge with a high value (more than – 30 mV) that indicated the stabilized liposomal particles in system. All formulations could entrap GA in system effectively with the entrapment efficiency of almost 100%. The formulation that provided high Cur entrapment in system may in LP2 which was composed of high hydrogenated lecithin and surfactants

Table 3. Characterization liposomal formulations, expressed as particles size, PdI value, ZP, and %EE

Formulations	Size (nm)*	PdI*	ZP (mV)*	% EE*	
				GA	Cur
LB1	157.40 ± 2.03[c]	0.36 ± 0.06[b]	-43.33 ± 0.96[a,b]	-	-
LB2	51.53 ± 0.12[a]	0.24 ± 0.01[a]	-28.33 ± 5.81[c]	-	-
LB3	223.87 ± 16.05[d]	0.90 ± 0.13[d]	-47.80 ± 0.44[a]	-	-
LB4	70.67 ± 5.03[b]	0.42 ± 0.04[c]	-36.17 ± 0.45[b]	-	-
LP1	231.87 ± 2.83[b]	0.30 ± 0.04[b]	-40.60 ± 0.61[b]	99.91 ± 0.03[b,c]	77.13 ± 0.02[d]
LP2	288.07 ± 1.89[b]	0.56 ± 0.08[c]	-49.17 ± 1.00[a]	99.90 ± 0.05[c]	95.43 ± 0.00[a]
LP3	804.27 ± 74.71[c]	0.69 ± 0.02[d]	-30.95 ± 0.15[d]	99.92 ± 0.07[b]	89.99 ± 0.01[c]
LP4	130.07 ± 0.40[a]	0.19 ± 0.01[a]	-36.50 ± 1.04[c]	99.99 ± 0.11[a]	92.93 ± 0.01[b]

*Lowercase letters indicate significant differences in blank liposome group (LB) and liposomal encapsulation group (LP) ($P < 0.05$) in terms of size, PdI, zeta potential and %EE investigation.

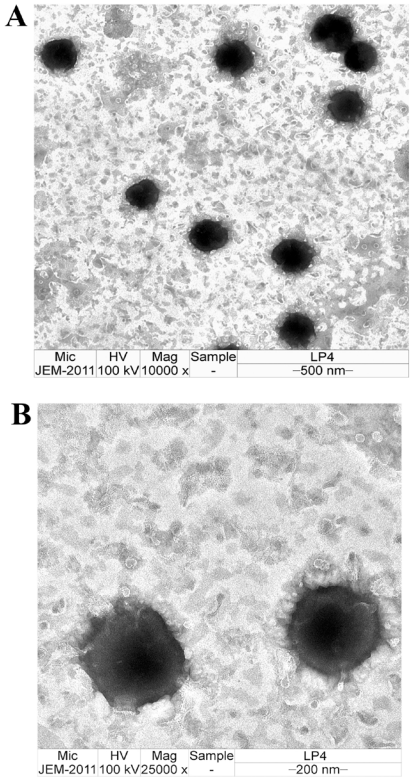

Figure 4. TEM images. The morphology of liposomes LP4 containing GA and Cur curcumin at magnification of **(A)** 10,000× and **(B)** 25,000×.

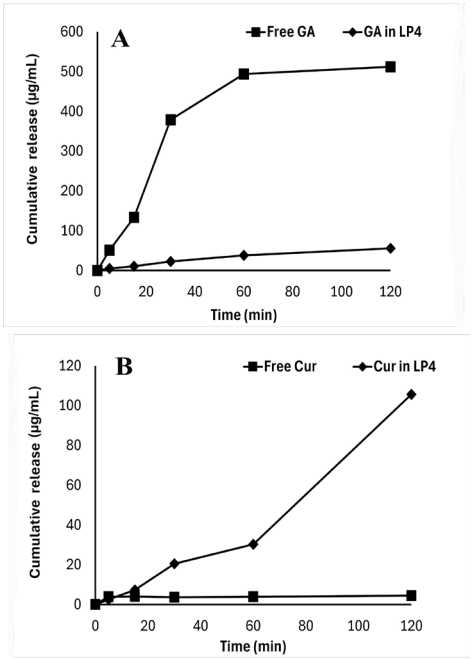

Figure 5. *In vitro* release. (A) Release profile of free GA compared with GA in LP4 and **(B)** free Cur in comparison with Cur in LP4 compared with Cur in LP4.

contents, followed by LP4, LP3, and LP1, respectively.

3.6. Liposomal morphology

From the results of viscosity, appearance characterization, particle size analysis, and %EE, LP4 was considered as the best system to entrapped GA and Cur with a small, stabilized particle size. Thus, LP4 was selected to study in the next step.

The morphology of the liposome LP4 containing GA and Cur investigated under TEM was shown as TEM images. The liposomal particles were a spherical dark shape with a good distribution as shown in Figure 4A. An unilamellar liposomes, a vesicle with a single lipid layer, were observed at a high magnification (25,000×) as shown in Figure 4B. The particle size from TEM images (approximately 200 nm) resembled that conducted from Zetasizer. Some large particles that were observed may be attributed to the dehydration process in sample preparation which resulted in particle aggregation.

3.7. Release study

The release study was performed under the sink conditions. 0.5% Tween 80 in PBS pH 7.4 was used as medium in the *in vitro* release study. The results from this study were shown in Figure 5, demonstrated a slow sustained releasing pattern of GA and Cur from LP4. GA from LP4 gradually released at 15 min with approximately 2% released, followed by a sustained release. Meanwhile, Cur from LP4 demonstrated biphasic release pattern. The release of GA and Cur from

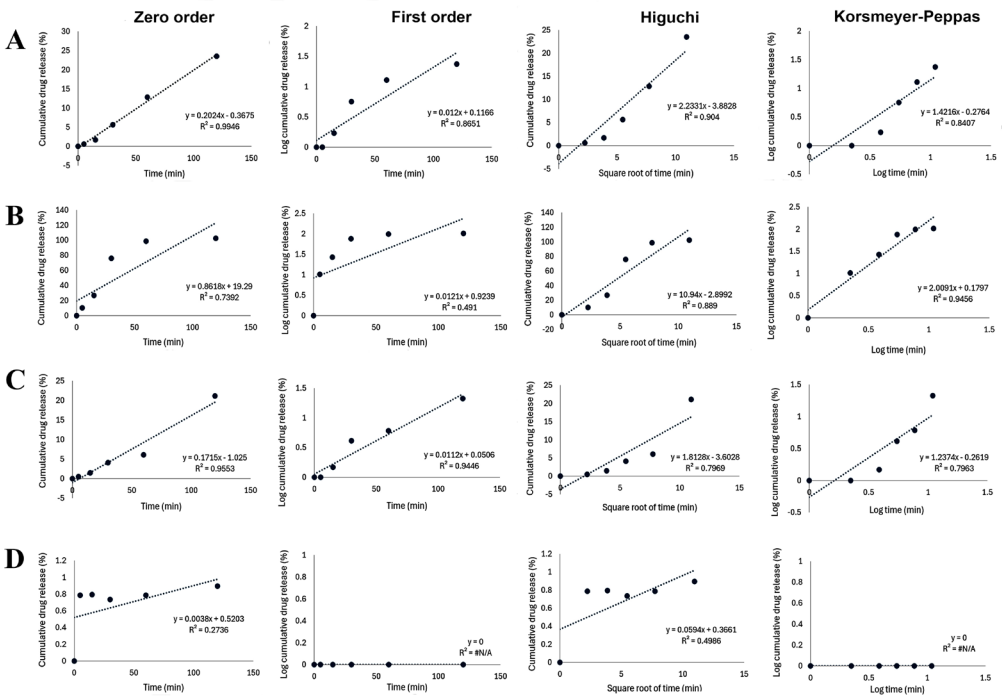

Figure 6. The kinetics of drug release. Release kinetics plot of **(A)** GA in LP4, **(B)** free GA, **(C)** Cur in LP4, and **(D)** free Cur using various kinetic models.

Table 4. Rate of GA and Cur release with various kinetic mechanisms

Samples	Kinetic releasing model							
	Zero-order		First-order		Higuchi		Korsmeyer-Peppas	
	k	R^2	k	R^2	k	R^2	k	R^2
GA in LP4	0.0926	0.9584	0.0097	0.7465	1.0787	0.9706	1.2023	0.7975
Free GA	0.8618	0.7392	0.0121	0.491	10.94	0.889	2.0091	0.9456
Cur in LP4	0.1945	0.9553	0.0123	0.8867	1.9509	0.7969	1.3663	0.7609
Free Cur	0.0038	0.2736	N/A	N/A	0.0594	0.4986	N/A	N/A

N/A: Not Applicable.

liposomes (LP4) at the end of the experiment (120 min) were similarly found to be 11.14 ± 0.10% and 0.90 ± 0.02%, respectively. Whereas, free GA possessed a short initial burst release of 379 ± 0.26 µg/mL (76%) after 30 min and then subsequently sustained released to 100% after 120 min and free Cur was released less than 10 µg/mL along the study time. These results suggest that encapsulation in LP4 effectively modulates the release of both GA and Cur, providing a more controlled and sustained delivery compared to their free forms.

In this study, the release mechanisms of GA and Cur from liposomes, compared to their free forms, were evaluated using four mathematical models: Zero-order, First-order, Higuchi, and Korsmeyer-Peppas. The most suitable model was determined based on the correlation coefficient (R^2) obtained from linear regression analysis for each model, as shown in Figure 6 and Table 4. After 120 min of the release study, the results indicated that the release profile of GA from liposomes followed the Higuchi model, with a release rate constant (k) of 1.0787. In contrast, Cur from liposomes exhibited a release behavior consistent with the Zero-order model, with a slower release rate characterized by a k value of 0.1945. For the free forms, both GA and Cur followed the Higuchi model, suggesting that the release mechanism was governed by Fickian diffusion. Furthermore, free GA was released more rapidly than free Cur, due to its smaller molecular size and higher hydrophilicity.

While the release mechanism analysis based on the R^2 values of various models provides valuable insights, it may not offer a comprehensive understanding of the underlying processes. Moreover, the study duration may be insufficient to capture the complete release profile. Therefore, further investigations are necessary to elucidate the complex interplay of factors governing drug release kinetics from liposomal formulations. Advanced techniques, such as molecular-level simulations, could be employed to provide a more detailed and nuanced understanding of the release phenomena.

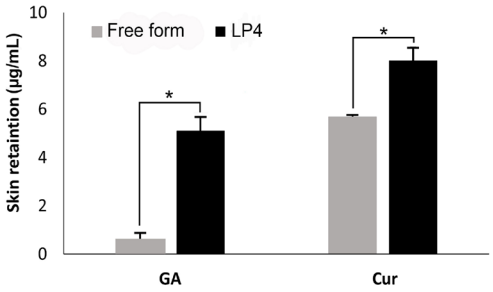

Figure 7. The accumulated compounds in the membrane that were obtained from Franz diffusion cell method. GA and Cur retention in skin membrane results 480 min after the *in vitro* skin permeation study. The quantitative analysis was employed by comparing free form compounds with compounds loading in LP4 (*$P < 0.05$).

3.8. Skin penetration and skin retention studies

The result of skin penetration study obtained from Franz diffusion cell method was found that only free GA and GA in LP4 can penetrate though the membrane to receiver chamber since 5 min of the study with concentration of 2.03 ± 0.27 µg/mL, whereas the initial penetration of GA in LP4 through the receiver chamber was 1.62 ± 0.29 µg/mL. The in-tact GA was rapidly absorbed more GA in LP4 and increased in a time-dependent manner. GA was found in the receiver chamber with concentration of 2.03 ± 0.27, 2.51 ± 0.11, 4.47 ± 0.23, 8.28 ± 1.08, 11.11 ± 0.88, 15.96 ± 0.59, 22.36 ± 1.47, and 29.63 ± 2.18 µg/mL at 5, 15, 30, 60, 120, 240, 360, and 480 min, respectively. Whereas Cur both in LP4 and free form were not found in the medium receiver chamber. However, the results from skin retention study as shown in Figure 7 demonstrated that liposome enhanced GA and Cur penetrated deep skin and retained in the skin significantly ($P < 0.05$). The free GA and free Cur were retained in membrane or skin with a concentration of 0.59 ± 0.07 µg/mL and 5.69 ± 0.29 µg/mL. Whereas GA and Cur in LP4 were found higher in skin than free form with the concentration of 5.08 ± 0.61 µg/mL and 8.00 ± 0.55 µg/mL, respectively.

4. Discussion

Various mechanisms of antioxidant activities have been extensively investigated to characterize how antioxidants against free radicals and oxidative damage. The crucial mechanisms include free radical scavenging, catalysis of ROS or NOS generation by transition metals like iron or copper, and inhibition of lipid peroxidation that affected the chain reaction initiated by free radicals leading to the degradation of polyunsaturated fatty acids in lipid at cell membranes and lipoproteins (*21*). A recent study possessed that GA and Cur were the potential antioxidant with mechanism of scavenging ROS radicals obtained from DPPH assay, inhibit NOS radicals obtained from NO scavenging assay, and inhibition of lipid peroxidation more than other samples, that may be attributed to the strong hydrogen-donating capacity, resulting in effectively binding the free radicals (*22*). The previous study has reported the benefits of GA and Cur combination for use as natural antioxidants with synergistic effects (*23*). However, the application for skin of GA and Cur in binding form were limited caused by their different physiochemical properties, particularly their contrasting of hydrophilicity and lipophilicity.

Drug delivery systems such as liposomal formulations, nanoemulsions, and solid lipid nanoparticles have been widely used to deliver hydrophilic- and lipophilic-compounds through deep skin (*24*). The previous studies have been investigated and developed GA, a hydrophilic compound and Cur, a lipophilic compound co- delivery system such as GA and Cur loaded chitosan microsphere (*25*) and Cur loaded cyclodextrin-conjugated GA (*26*). Liposomes are a promising delivery system due to their ability to encapsulate both hydrophilic and hydrophobic molecules within their lipid bilayer structure, which is formed by phospholipids or hydrogenated lecithin (*27*). This system is thus employed to encapsulate GA and Cur in this study, expected to apply for skin products. The typical composition of liposomes, otherwise phospholipid, are cholesterol, surfactants, and solubilizers to modify liposomal vesicle properties including size, stability, flexibility, and drug loading capacity (*28*). Non-ionic surfactants, such as polysorbate 80, polysorbate 20, and sorbitan oleate, are commonly utilized in liposome formulations for skin applications due to their less toxicity (*29*). These surfactants thus selected employed in the present study. High hydrogenated lecithin and surfactants content lead to high viscosity and rigid structure (*30,31*) which was revealed to this study. LB2, LB3, LP2, and LP3 were composed of high content of hydrogenated lecithin and surfactants in formulation demonstrate high viscosity. Moreover, this study found that the content ratios of hydrogenated lecithin, cholesterol, surfactants, and solubilizers in system significantly influenced size, size distribution, zeta potential (ZP) and compound-entrapments conformed to the reported studies by Pande S and Chen *et al*. (*32,33*). The formulation composed of 0.5% hydrogenated lecithin, 0.2% cholesterol, 5% ethylexyl palmitate, 2.5% di-propylene glycol, 1% tocopheryl acetate, 8% polysorbate 80, 10% sorbitan oleate, and 72.05% DI water was the most suitable ratio that provide homogenous appearance, small particle size with stabilized system with high value of ZP (> -30 mV), high entrapment efficiency both GA and Cur. The zeta potential of liposomal vesicles was negative, attributed to the negative charge obtained from the phosphate group of hydrogenated lecithin (*34,35*).

The release of a formulation is a critical factor influencing efficacy, rate and extent of active ingredient delivery to the target site. This study was done by observing in 120 min according to the further application as topical product same as the release study anti-inflammatory topical formulations (*36*). The results in

the resent study found that LP4 exhibited control release of GA and Cur within the bilayer of liposomes typically exhibits a burst release upon disruption of the liposomal structure, followed by a sustained release phase. Then, GA which is expected to be in the hydrophilic core of vesicle demonstrate a sustained release (*37,38*). GA in LP4, free form of GA and Cur employed the Higuchi kinetic model that possessed the release follows Fick's law of diffusion. This model describes drug diffusion through a homogeneous matrix or solution, driven by a concentration gradient (*39*). The drug release rate depends on the square root of time. Similar release patterns have been observed in matrix-based or solution-based drug delivery systems (*19,40*). Whereas, the release of Cur from LP4 following a Zero-order kinetic model, means that the release rate is constant over time. This appearance might depend on the amount of Cur remaining in the liposome and the limited released into medium, because the cumulative release amount does not increase over the duration of study. These results revealed a previous study that reported abiraterone acetate, hydrophobic drug, loaded liposome found to be sustained release and fit to the Zero-order model (*41*).

The negative charge of particles enhances their skin permeation by promoting electrostatic interactions with the skin negatively charged surface, thereby facilitating penetration, and improving drug localization within the skin layers (*42*). The present study demonstrated that liposomes could enhance Cur skin permeation and skin retention effectively. There was revealed to previous report that curcumin loaded soybean phospholipid-base liposome promoted drug permeation and deposition (*44*). Moreover, the results showed that free GA could penetrate and reach the receiver chamber faster than GA in liposome, and this phenomenon may be due to the molecular properties and the structure of the liposome that provides a controlled release system. GA, a small hydrophilic molecule (Mw ~170 Da), which is within the range favorable for skin absorption *via* transcellular pathway. Whereas liposomes, with their lipophilic bilayer structure, are better suited for permeation through the lipid-rich tight junctions between corneocyte cells, facilitating localized and sustained delivery (*7,44,45*).

In conclusion, liposome-encapsulated gallic acid and curcumin offer significant advantages for topical antioxidant skincare products. Their improved skin penetration facilitates better absorption into deeper layers leading to enhancing effectiveness. Controlled release provides sustained antioxidant protection over time. Encapsulation minimizes direct skin contact, potentially reducing irritation risk. These benefits promising this system for both cosmetic and therapeutic skincare applications.

Acknowledgements

The authors are grateful to the Faculty of Pharmacy, Chiang Mai University for their support.

Funding: This work was supported by a grant from CMU Junior Research Fellowship program (Grant number : JRCMU2566R_098).

Conflict of Interest: The authors have no conflicts of interest to disclose.

References

1. Turkan I. ROS and RNS: Key signaling molecules in plants. J Exp Bot. 2018; 69:3313-3315.
2. Chen J, Liu Y, Zhao Z, Qiu J, Oxidative stress in the skin: Impact and related protection. Int J Cosmet Sci. 2021; 43:495-509.
3. Bickers DR, Athar M. Oxidative stress in the pathogenesis of skin disease. J Invest Dermatol. 2006; 126:256-2575.
4. D'Orazio J, Jarrett S, Amaro-Ortiz A, Scott T. UV radiation and the skin. Int J Mol Sci. 2013; 14:12222-12248.
5. Sivaranjani N, Rao SV, Rajeev G. Role of reactive oxygen species and antioxidants in atopic dermatitis. J Clin Diagn Res. 2013; 7:2683-2685.
6. Tadapaneni RK. Effect of high pressure processing & dairy on the antioxidant activity of strawberry based beverages. J Agric Food Chem. 2012; 60:5795-5802.
7. Phatale V, Vaiphei KK, Jha S, Patil D, Agrawal M, Alexander A. Overcoming skin barriers through advanced transdermal drug delivery approaches. J Control Release. 2022; 351:361-380.
8. Hoang HT, Moon JY, Lee YC. Natural antioxidants from plant extracts in skincare cosmetics: Recent applications, challenges and perspectives. Cosmetics. 2021; 8:8040106.
9. Kahkeshani N, Farzaei F, Fotouhi M, Alavi SS, Bahramsoltani R, Naseri R, Momtaz S, Abbasabadi Z, Rahimi, R, Farzaei MH, Bishayee A. Pharmacological effects of gallic acid in health and diseases: A mechanistic review. Iran J Basic Med Sci. 2019; 22:225-237.
10. Liu S, Liu J, He L, LiuL, Cheng B, Zhou F, Cao D, He Y. A comprehensive review on the benefits and problems of curcumin with respect to human health. Molecules. 2022; 27:2714400.
11. Bangar SP, Chaudhary V, Sharma N, Bansal V, Ozogul F, Lorenzo JM. Kaempferol: A flavonoid with wider biological activities and its applications. Crit Rev Food Sci Nutr. 2023; 63:9580-9604.
12. Dossou SSK, Xu F, Dossa K, Zhou R, Zhao Y, Wang L. Antioxidant lignans sesamin and sesamolin in sesame (*Sesamum indicum* L.): A comprehensive review and future prospects. J Integr Agric. 2023; 22:4-30.
13. Souto EB, Fangueiro JF, Fernandes AR, Cano A, Sanchez-Lopez E, Garcia ML, Severino P, Paganelli MO, Chaud MV, Silva AM. Physicochemical and biopharmaceutical aspects influencing skin permeation and role of SLN and NLC for skin drug delivery. Heliyon. 2022; 8:e08938.
14. Pierre MBR, Dos Santos Miranda Costa I, Liposomal systems as drug delivery vehicles for and transdermal applications. Arch Dermatol Res. 2011; 303:607-621.
15. Figueroa-Robles A, Antunes-Ricardo M, Guajardo-Flores D. Encapsulation of phenolic compounds with liposomal improvement in the cosmetic industry. Int J Pharm. 2021; 593:120125.
16. Phumat P, Chaichit S, Potprommanee S, Preedalikit W,

Sainakham M, Poomanee W, Chaiyana W, Kiattisin K. Influence of *Benincasa hispida* peel extracts on antioxidant and anti-activities, including molecular docking simulation. Foods. 2023; 12:12193555.
17. Jagetia GC, Baliga MS. The evaluation of nitric oxide scavenging activity of certain Indian medicinal plants *in vitro*: A preliminary study. J Med Food. 2004; 7:343-348.
18. Elzaawely AA, Xuan TD, Koyama H, Tawata S. Antioxidant activity and contents of essential oil and phenolic compounds in flowers and seeds of *Alpinia zerumbet* (Pers.) B.L. Burtt. & R.M. Sm. Food Chem. 2007; 104:1648-1653.
19. Okonogi S, Phumat P, Khongkhunthian S, Chaijareenont P, Rades T, Müllertz A. Development of self-nanoemulsifying drug delivery systems containing 4-allylpyrocatechol for treatment of oral infections caused by *Candida albicans.* Pharmaceutics. 2021; 13:167.
20. Nitthikan N, Leelapornpisid P, Naksuriya O, Intasai N, Kiattisin K. Multifunctional biological properties and topical film forming spray base on *Auricularia polytricha* as a natural polysaccharide containing brown *Agaricus bisporus* extract for skin hydration. Cosmetics. 2023; 10:10050145.
21. Jomova K, Raptova R, Alomar SY, Alwasel SH, Nepovimova E, Kuca K, Valko M. Reactive oxygen species, toxicity, oxidative stress, and antioxidants: Chronic diseases and aging. Arch Toxicol. 2023; 97:2499-2574.
22. Lobo V, Patil A, Phatak A, Chandra N. Free radicals, antioxidants and functional foods: Impact on human health. Pharmacogn Rev. 2010; 4:118-126.
23. Naksuriya O, Okonogi S. Comparison and combination effects on antioxidant power of curcumin with gallic acid, ascorbic acid, and xanthone. Drug Discov Ther. 2015; 9:136-141.
24. Stefanov SR, Andonova VY. Lipid nanoparticulate drug delivery systems: Recent advances in the treatment of skin disorders. Pharmaceuticals. 2021; 14:4111083.
25. Ricci A, Stefanuto L, Gasperi T, Bruni F, Tofani D. Lipid nanovesicles for antioxidant delivery in skin: Liposomes, ufasomes, ethosomes, and niosomes. Antioxidants. 2024; 3:1516.
26. Omrani Z, Dadkhah Tehrani A. New cyclodextrin-based supramolecular nanocapsule for codelivery of curcumin and gallic acid. Polym Bull 2020; 77:2003-2019.
27. Akbarzadeh A, Rezaei-Sadabady R, Davaran S, Joo SW, Zarghami N, Hanifehpour Y, Kouhi M, Nejati-Koshki K. Liposome: Classification, preparation, and applications. Nanoscale Res Lett. 2013; 8:102.
28. Jiang Y, Li W, Wang Z, Lu J. Lipid-based nanotechnology: Liposome. Pharmaceutics. 2024; 34:16010034.
29. Lémery E, Briançon S, Chevalier Y, Bordes C, Oddos T, Gohier A, Bolzinger MA. Skin toxicity of surfactants: Structure/toxicity relationships. Colloids Surf A Physicochem Eng Asp. 2015; 469:166-179.
30. Rahman MA, Hussain A. Lecithin-microemulsion based organogels as topical drug delivery system (TDDS). Int J Curr Res Rev. 2011; 3:22-33.
31. Nazdrajic S, Bratovcic A, Alibegic D, Micijevic A, Mehovic M, The effect of mixed surfactants on viscosity, pH and stability of synthesized liquid soaps. Int J Anal Chem. 2024; 14:31-36.
32. Pande S. Factors affecting response variables with emphasis on drug release and loading for optimization of liposomes. Artif Cells Nanomed Biotechnol. 2024; 52:334-344.
33. Shu Q, Wu J, Chen Q. Synthesis, characterization of liposomes modified with biosurfactant MEL-A loading betulinic acid and its anticancer effect in HepG2 Cell. Molecules. 2019; 24:3939.
34. Honary S, Zahir F. Effect of zeta potential on the properties of nano-drug delivery systems –A review (Part 1). Top J Pharm Res. 2013; 12:255-264.
35. de Toledo AMN, Silva NCC, Sato ACK, Picone CSF. A comprehensive study of physical, antimicrobial and emulsifying properties of self-assembled chitosan/lecithin complexes produced in aqueous media. Future Foods. 2021; 4:100083.
36. Burcea-Dragomiroiu GTA, Moroşan E, Popa DE, Niţă S, Rasit I, Panteli M, Golokhvast KS, Ginghină O. *In vivo* testing of the anti-inflammatory action of topical formulations containing cobalt complexes with oxicams. Public Health Toxicol. 2023; 3:1-9.
37. Harwansh RK, Deshmukh R, Shukla VP, Khunt D, Prajapati BG, Rashid S, Ali N, Elossaily GM, Suryawanshi VK, Kumar A. Recent advancements in gallic acid-based drug delivery: Applications, clinical trials, and future directions. Pharmaceutics. 2024; 16:16091202.
38. Fernández-Romero AM, Maestrelli F, Mura PA, Rabasco AM, González-Rodríguez ML. Novel findings about double-loaded curcumin-in-HPβcyclodextrin-in liposomes: Effects on the lipid bilayer and drug release. Pharmaceutics. 2018; 10:10040256.
39. Siepmann J, Peppas NA. Higuchi equation: derivation, applications, use and misuse. Int J Pharm. 2011; 418:6-12.
40. Costa P, Sousa Lobo JM. Modeling and comparison of dissolution profiles. Eur J Pharm Sci. 2001; 13:123-133.
41. Das S, Samanta A, Mondal S, Roy D, Nayak AK. Design and release kinetics of liposomes containing abiraterone acetate for treatment of prostate cancer. Sens Int. 2021; 2:100077.
42. Ogiso T, Yamaguchi T, Iwaki M, Tanino T, Miyake,Y. Effect of positively and negatively charged liposomes on skin permeation of drugs. J Drug Target. 2001; 9:49-59.
43. Chen Y, Wu Q, Zhang Z, Yuan L, Liu X, Zhou L. Preparation of curcumin-loaded liposomes and evaluation of their skin permeation and pharmacodynamics. Molecules. 2012; 17:5972-5987.
44. Zoabi A, Touitou E, Margulis K. Recent advances in nanomaterials for dermal and transdermal applications. Colloids Interfaces. 2021; 5:5010018.
45. Faber I, Pouvreau L, Jan van der Goot A, Keppler J. Modulating commercial pea protein gel properties through the addition of phenolic compounds. Food Hydrocoll. 2024; 154:110123.

Received January 2, 2025; Revised February 1, 2025; Accepted February 21, 2025.

**Address correspondence to:*
Pimpak Phumat, Department of Pharmaceutical Sciences, Faculty of Pharmacy, Chiang Mai University, Chiang Mai 50200, Thailand.
E-mail: pimpak.p@cmu.ac.th

Released online in J-STAGE as advance publication February 26, 2025.